Rotational State Effects in the Dissociative Recombination of H_2^+

V. Zhaunerchyk,[1] A. Al-Khalili,[1] R. D. Thomas,[1] W. D. Geppert,[1] V. Bednarska,[2] A. Petrignani,[2] A. Ehlerding,[1]
M. Hamberg,[1] M. Larsson,[1] S. Rosen,[1] and W. J. van der Zande[2]

[1]*Department of Physics, Albanova University Centre, Stockholm University, S106 91 Stockholm, Sweden*
[2]*Institute for Molecules and Materials, Radboud University Nijmegen, P.O. Box 9010, NL-6500 GL Nijmegen, The Netherlands*
(Received 31 January 2007; published 2 July 2007)

We have studied the dissociative recombination (DR) of molecular hydrogen ions with slow electrons over a range of collision energies from 0 to 400 meV. By employing a pulsed expansion source for rotational cooling and by exploiting superelastic collisions with near-0-eV electrons in a heavy ion storage ring for vibrational cooling, we observe a highly structured DR cross section, comparable to that reported for HD^+. Using *para*-hydrogen-enriched ion beams, we identify for the first time features in the DR cross sections attributed to $\nu = 0$, $J =$ even molecules (*para*-H_2) and $\nu = 0$, $J =$ odd (*ortho*-H_2) molecules, separately. Indications are given that *para* levels have different DR rate coefficients from *ortho* levels for the first four vibrational levels at near-0-eV collisions.

PACS numbers: 34.80.Ht

Dissociative recombination (DR) is an important process in weakly ionized media such as interstellar space, planetary atmospheres, and reactive plasmas. In DR, an electron collision with a molecular ion results in the breakup of the neutral molecule formed in the collision. The relevance of DR comes from its very high efficiency in the case of slow electrons; DR often determines the equilibrium concentration of slow electrons in plasmas. In the physical process underlying DR, an electron is captured into a neutral, doubly excited, molecular state or a vibrationally excited Rydberg state converging to the ionic ground state. These excited states, also called superexcited states, are not stable and dissociate on a time scale similar to that of autoionization. Autoionization competes with DR and changes the electron capture into an elastic electron scattering process, an inelastic scattering process, or, and relevant for the presented results, a superelastic scattering process [1]. The latter process leaves the molecular ion rovibrationally deexcited.

Molecular hydrogen is of special astrophysical relevance. The presence of nuclear spin divides molecular hydrogen into *para*-hydrogen ($I = 0$) and *ortho*-hydrogen ($I = 1$). Because of symmetry reasons, *para*-hydrogen has only even rotational levels, whereas *ortho*-hydrogen has only odd rotational levels in the neutral and ionic electronic ground states. As *para*- and *ortho*-hydrogen interconvert extremely slowly, different rotationally dependent DR rates could result in selective enrichment of *para*-H_2^+ or *ortho*-H_2^+ under the conditions present in interstellar space. The molecular hydrogen ion deserves detailed study also for fundamental reasons. Experiment and theory still have not converged in all aspects of the details. At low electron-collision energies, and for the first five vibrational levels in H_2^+, the doubly excited $Q_1{}^1\Sigma_g^+(2p\sigma_u)^2$ state is the major capture and dissociation channel. The crossing point between the molecular ion ground state and the doubly excited neutral state suggests a small recombination rate

coefficient with low energy electrons for the vibrational ground state (see Fig. 1). Indeed, the DR rate coefficient is known to increase significantly when going from $\nu = 0$ to $\nu = 1$ [2]. Results reported from beautiful experiments at the TSR storage ring have quantified this effect for H_2^+ as well as for HD^+ and provided vibrational state-specific DR rate coefficients [3,4]. Superelastic collisions (SECs) were found to deexcite H_2 molecular ions efficiently, resulting in a nearly pure H_2^+ ($\nu = 0$) ion beam. When the vibrational quantum number is increased, the recombination rate coefficient is anticipated to increase significantly again at the $\nu = 5$ state and higher. The reason for this is that the wave function overlap with the higher lying doubly excited Q_1
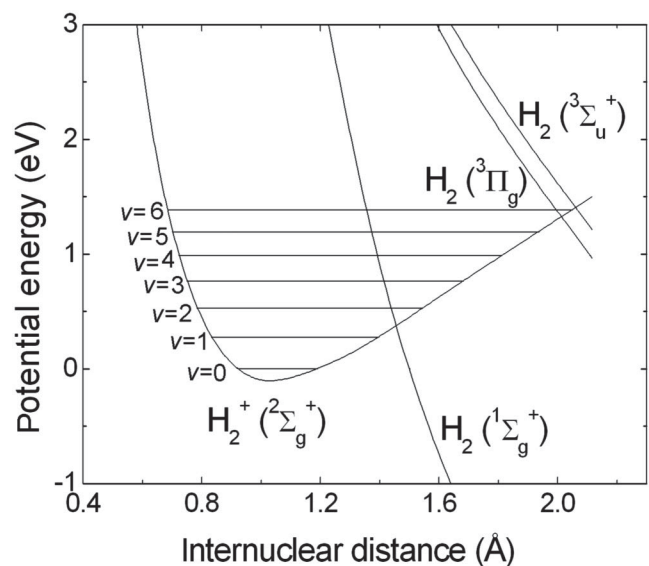

FIG. 1. The ground state of H_2^+ and the three lowest Q_1 states for neutral H_2. The curves are adopted from Guberman [19]. The positions of the first seven vibrational levels in H_2^+ are also indicated.

states of molecular hydrogen suddenly increases (see Fig. 1). These effects have also been observed in DR experiments at heavy ion storage rings [5]. Dynamics in storage ring experiments on the level of rotational states have not been reported for H_2^+. Upon switching to the isotopologue HD^+, this ion cools through infrared radiation with sufficient efficiency that a vibrationally cold ion beam ($\nu = 0$ only) is formed within a second. In the case of hydrogen, H_2^+, these infrared modes are forbidden, and the vibrational distribution should be measured in the experiment to understand what is occurring. Vibrational state distributions of hydrogen ion beams can be determined with great accuracy, for example, with dissociative charge transfer on alkali atoms [6]. At the TSR, a Coulomb explosion imaging (CEI) experiment has been installed to provide direct information on the vibrational populations of the ions in the ring [7]. In the present storage ring experiment, an imaging detector (ID) has been implemented to measure the vibrational populations indirectly. The spectrum from an ID measures the relative vibrationally resolved DR product distribution α_i, which are proportional to the vibrational populations p_i, multiplied by the vibrationally selective rate coefficient k_i: $\alpha_i = p_i k_i / \Sigma p_i k_i$. These data are plotted in Fig. 2.

The experiment reported here has been performed in the heavy ion storage ring CRYRING [8]. We have employed a pulsed discharge expansion source [9] loaded with a mixture of H_2 (<10%) and Ne at a pressure of 2 bar. Ion-molecule reactions between Ne and H_2^+ remove part of the vibrational states above $\nu = 1$ in the reaction $H_2^+(\nu > 1) + Ne \rightarrow NeH^+ + H$ [10]. The supersonic expansion should further rotationally cool the molecular ions. We
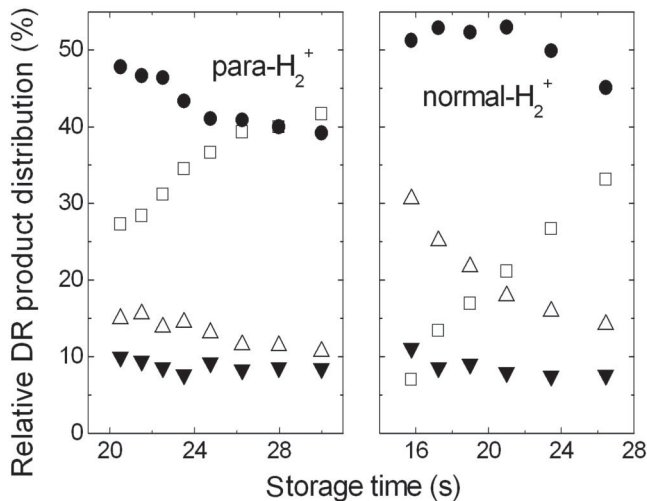

FIG. 2. The relative vibrationally resolved DR product distribution α_i for the first four vibrational levels ($i = 0$–3), $\nu = 0$ ($\square$), $\nu = 1$ ($\bullet$), $\nu = 2$ ($\triangle$), and $\nu = 3$ ($\blacktriangledown$), at various times after injection for both para-H_2^+ and normal H_2^+ as deduced from a position-sensitive fragment-imaging technique. The ion beam energy was 15 MeV.

note that a rotational temperature of the ions of 30 K means that the ion beam would consist of approximately 25% para-H_2^+ ground state ions ($J = 0$) and 75% ortho-H_2^+ ground state ions ($J = 1$), while in a pure para-H_2^+ beam only $J = 0$ should be populated [9]. The para-hydrogen gas was produced off-line and was checked to have a purity of 99%. In our experiment, the ions are extracted from the ion source by a potential of 20 kV and then accelerated in the storage ring to translational energies of 8 and 15 MeV. In the experiments at higher energies, a new source of rovibrational heating was found; only the 8 MeV beam-energy experiments provided sufficient cooling to resolve detailed structures in the DR rate coefficient spectra. Inside an electron cooler, the ions interact during each passage with the highly monoenergetic electron beam over a length of 0.85 m. The electron-collision energy E can be continuously tuned from near 0 eV to any required collision energy by changing the laboratory electron energy. At low electron-collision energies, the estimated collision energy spread is 2.5 meV. In the electron-interaction region, the superelastic collisions and the DR reactions take place. Neutral products are detected by an ion implanted silicon detector (IISD) or on the ID [11]. The IISD is used for the determination of the DR rate, whereas the ID is used for obtaining information on the vibrational distribution of the ion beam. The distance between the fragments on the detector is a measure for the initial vibrational state. The product distributions as a function of time and the DR cross sections as a function of electron-collision energy were obtained in separate experiments.

Figure 3 presents the most important result from the present research. The figure plots the collision energy-dependent DR rate coefficient after storage times of 3 and 17 s for both normal and para-hydrogen. This experiment was performed at an ion beam energy of 8 MeV. Note that, instead of the cross section, we plot the product of the rate coefficient and the square root of the collision energy on the abscissa. We have chosen this representation to avoid logarithmic scales connected to the $1/\sqrt{E}$ dependency of the DR rate coefficient at small collision energies. The observed rates after 17 s are much smaller that those after 3 s. At early times, the rate coefficients as a function of energy are almost structureless. The observed DR rates after 17 s of cooling and superelastic collisions reveal much more structure than the spectra taken at an earlier storage time. If the rotational distribution generated in the ion source is not changed during extraction and acceleration, it is possible that all of these observed structures are due to a single quantum state in para-hydrogen ($I = 0$, $J = 0$, $\nu = 0$) and due to two quantum states in normal hydrogen ($I = 0$, $J = 0$, $\nu = 0$) and ($I = 1$, $J = 1$, $\nu = 0$). It is, of course, possible that SECs keep the rotational population cold. Moreover, the spectrum obtained for vibrationally cooled HD^+ [12] has similarities with the spectrum of normal H_2^+ after 17 s of storage in the ring
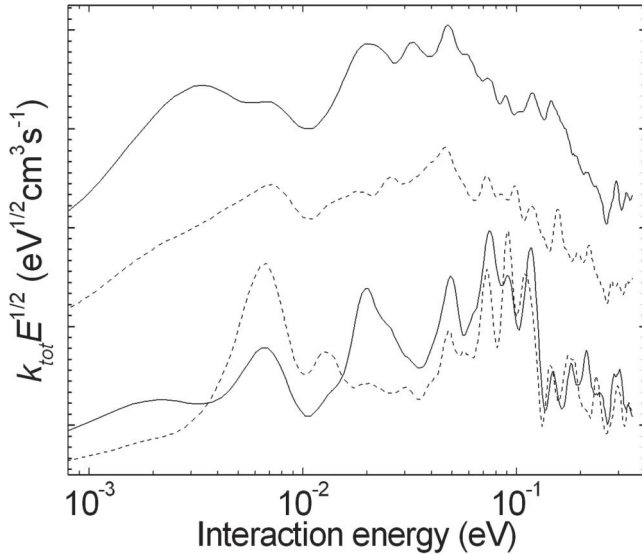
FIG. 3. The rate coefficient k_{tot} multiplied by the square root of the interaction energy $E^{1/2}$ measured after a storage time of 3 (two upper curves) and 17 s (two lower curves) for an ion beam energy of 8 MeV. The results for both *para*-H_2^+ (dashed line) and normal H_2^+ (solid line) are plotted. Although the decrease in the rate coefficients with storage is real, the rate coefficients of *para*- and normal hydrogen cannot be compared absolutely, and so no scale is given.

(Fig. 3). Since the HD$^+$ molecule has a permanent dipole moment, its rotational distribution corresponded to a temperature of 300 K where the $J = 0$–4 states are significantly populated. This observation supports the assertion that the spectrum measured for normal-H_2^+ after 17 s containing both features of even and odd rotational quantum states originate mostly from the vibrational ground state. In comparing the normal-hydrogen spectrum with that of *para*-hydrogen, significant differences are observed. The resonance at 6 meV has a width of about 2 meV and is predominantly a *para*-hydrogen feature, whereas the peaks at ≈ 2 and ≈ 18 meV are predominantly *ortho*-hydrogen features. Other features are observed in both the *para*- and the normal hydrogen spectra. Many of the peaks have widths limited by the instrumental resolution. The rate coefficient spectra of *para*-H_2^+, normal H_2^+, and HD$^+$ all reveal a sudden drop in the rate at about 0.14 eV, above which strong peaks are absent.

The fact that $v = 0$ ions have a DR spectrum with more structure may be attributed to the small cross section by the direct mechanism. As the crossing of the doubly excited neutral state for low energy electrons is above the $v = 1$ level, the direct Franck-Condon overlap between the ionic $v = 0$ state and the doubly excited continuum is very small. The indirect mechanism [13], in which vibrationally excited Rydberg state levels are formed and which are subsequently dissociated by the doubly excited state, gives

rise to resonances. In earlier theoretical calculations, Rydberg resonances often appeared as window resonances where the cross section was reduced [14,15], which was observed experimentally [16,17]. The current spectrum suggests that resonances give rise to local enhancements of the DR rate at specific energies. Although more recent calculations by Takagi reveal this effect as well, unfortunately no quantitative agreement is found with our data regarding the position of the observed resonances [18]. The fact that $v > 1$ ions do not show detailed Rydberg structure may be understood by the dominance of the direct mechanism for these ions: The continuum has no detailed structure, and the rate coefficient has a more smooth dependence on the collision energy. Since the resonances are attributed to the presence of molecular Rydberg states, the peak positions may help to identify the vibrational state and the Rydberg state involved.

Figure 4 plots the time dependence of the DR rate coefficient k_{tot} for a collision energy of 0 (± 0.002) eV measured at the ion beam energy of 15 MeV for both normal and *para*-hydrogen. The deduced rate coefficient for normal H_2^+ is very close to the values obtained at the TARN II storage ring [1]; the comparison is appropriate since their experimental conditions and resolution are very similar to those in CRYRING. The decrease in k_{tot} is attributed to changes in the vibrational population, in particular, to the deexcitation of H_2^+ ions through the SEC process. Our results for normal hydrogen and *para*-hydrogen are not identical. A shift in time of one of the curves is not sufficient to obtain quantitative agreement. We conclude that the rates for the SEC and the DR process are different for *para*-H_2^+ and normal (*ortho*-)H_2^+ and hence depend on the rotational quantum number. Using six observations of the relative product distributions for normal hydrogen and eight for *para*-hydrogen at different storage
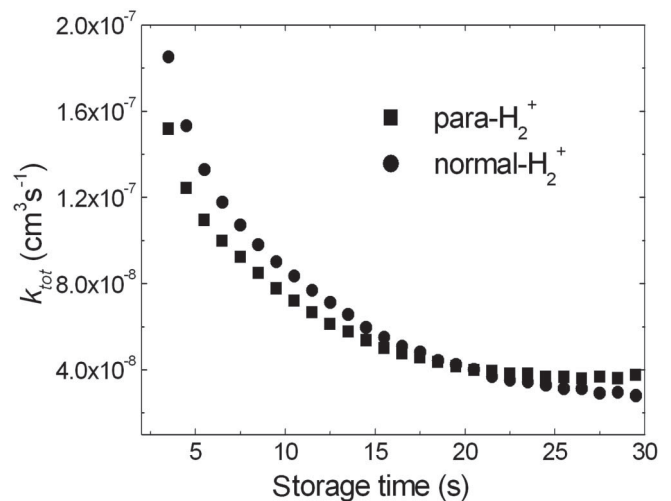

FIG. 4. The absolute total rate coefficients are shown both for *para*-H_2^+ (■) and normal H_2^+ (●) versus a storage time. The ion beam energy is 15 MeV.

TABLE I. The absolute DR rate coefficients for the first four vibrational states of *para-* and normal hydrogen obtained at near-0-eV interaction energy (all rate coefficients are written in units 1×10^{-8} cm^3 s^{-1}). The error bars present statistical uncertainties in the imaging data; however, for some rate coefficients, they were found to be very small and, therefore, are not presented here. All measured rate coefficients also have systematic uncertainty which can be as high as 15%.

	$\nu = 0$	$\nu = 1$	$\nu = 2$	$\nu = 3$
Para-H$_2^+$	2.7	6.04 ± 1.22	3.64 ± 0.87	3.73 ± 0.96
Normal H$_2^+$	1.42	11.5 ± 2.76	13.7	1.63 ± 0.56

times, we were able to deduce the rate coefficients for the first four vibrational levels using a least squares optimization procedure and Eq. (1):

$$\frac{1}{k_{\text{tot}}(t)} = \sum_{j=0}^{3} \frac{\alpha_j(t)}{k_j}. \quad (1)$$

Table I lists the vibrational rate coefficients for both *para-* and normal hydrogen. Despite the different experimental conditions in the CRYRING and TSR storage rings, the rate coefficients we report for normal H$_2^+$ ($\nu = 0$–2) are in very good agreement with those reported by Krohn [3]. The rate coefficients for *para*-H$_2^+$ are significantly different to those of normal H$_2^+$. We must conclude that in a small system such as hydrogen the change in going from $J = 0$ (*para*) to $J = 1$ (*ortho*) has a significant impact on the DR at 0 eV collisions. Our observation that the 0 eV rate coefficients for *para-* and normal hydrogen are different is of great interest. Formally, these differences may be due to the different nuclear spin and/or the rotational degree of freedom. A direct effect of nuclear-spin and hyperfine interactions seems unlikely due to the very small energy differences involved. An effect due to changes in rotational energy is more likely, since these differences in energy are much greater: The energy difference between the $J = 0$ and $J = 1$ level is 60 cm^{-1} (≈ 7.5 meV). Still, in view of the potential energy diagram and the physics of the direct mechanism, an energy difference of only 60 cm^{-1} also seems small. Significant variations are expected only over a vibrational spacing of 2190 cm^{-1}. Of course, resonance phenomena may affect rates at specific energies, and, since we observe the effects of electron collisions at 0 eV only, the *para-ortho* differences may be due to these resonances.

The observations and results presented here combine experiments taken at ion beam energies of 8 and 15 MeV. The higher energy was chosen to benefit from higher electron currents resulting in a higher rate of SEC and, hence, a faster cooling of the vibrational degree of freedom. We concluded, however, that for the highest ion

beam energy some vibrational reheating was occurring as deduced from the observed product distance distributions (Fig. 2) and the absence of clear structure in the DR rate coefficient spectra. So far, the source of the vibrational reheating has not been identified. Because of the presence of reheating the imaging data obtained at 15 MeV beam energy could not be used to derive the SEC rate coefficients.

Experiments with heavy ion storage rings have revealed many details on molecular hydrogen thanks to their intrinsic high resolving power in collision energy and due to the introduction of imaging techniques that allow identification of the vibrational state of the molecular ions in the experiment either directly, as in CEI, or through detection of the DR fragments themselves. The combination of these techniques made it possible to determine vibrational state-specific DR rate coefficients as well as to identify many intriguing effects regarding SEC and the dissociation behavior in the DR process. As all techniques still lack rotational resolution, the effect of rotation has to be studied by changing the conditions in an ion source. In this study, the use of an expansion source and *para*-hydrogen made it possible to have significant control over the rotational populations. Naturally, the absence of rotationally resolved diagnostics prevents us from achieving the ideal situation in which conclusions for each rotational state can be drawn.

[1] T. Tanabe *et al.*, Phys. Rev. Lett. **83**, 2163 (1999).
[2] V. Ngassam *et al.*, Phys. Rev. A **68**, 032704 (2003).
[3] S. Krohn, Ph.D. thesis, Max-Planck-Institut für Kernphysik, Heidelberg, 2001.
[4] Z. Amitay *et al.*, Phys. Rev. A **60**, 3769 (1999).
[5] W. J. van der Zande *et al.*, Phys. Rev. A **54**, 5010 (1996).
[6] A. Petrignani *et al.*, J. Chem. Phys. **122**, 014302 (2005).
[7] R. Wester *et al.*, Nucl. Instrum. Methods Phys. Res., Sect. A **413**, 379 (1998).
[8] C. Strömholm *et al.*, Phys. Rev. A **54**, 3086 (1996).
[9] B. J. McCall *et al.*, Phys. Rev. A **70**, 052716 (2004).
[10] A. Sen *et al.*, J. Phys. B **20**, 1509 (1987).
[11] S. Rosén *et al.*, Hyperfine Interact. **115**, 201 (1998).
[12] A. Al-Khalili *et al.*, Phys. Rev. A **68**, 042702 (2003).
[13] J. N. Bardsley, J. Phys. B **1**, 365 (1968).
[14] K. Nakashima, H. Takagi, and H. Nakamura, J. Chem. Phys. **86**, 726 (1987).
[15] H. Takagi, J. Phys. B **26**, 4815 (1993).
[16] H. Hus *et al.*, Phys. Rev. Lett. **60**, 1006 (1988).
[17] P. Van der Donk *et al.*, Phys. Rev. Lett. **67**, 42 (1991).
[18] H. Takagi (private communication).
[19] S. L. Guberman, J. Chem. Phys. **78**, 1404 (1983).